

# Implementation of sliding control with washout filter in boost and buck converters

Esteban Flórez Urrego, Fredy E. Hoyos, John E. Candelo-Becerra

Department of Electrical Energy and Automation, Faculty of Mines, Universidad Nacional de Colombia Sede Medellín, Medellín, Colombia

---

## Article Info

### Article history:

Received Sep 1, 2025

Revised Mar 16, 2026

Accepted Apr 23, 2026

---

### Keywords:

Boost converter

Buck converter

DC-DC converter

Sliding mode control

Washout control

---

## ABSTRACT

This paper presents the analysis, design, and implementation of a two-stage power conversion system consisting of a boost converter and a buck converter. Both converters were controlled using a sliding-mode control based on a washout filter. The system was supplied with an alternating current (AC) voltage source that was rectified using a diode bridge. The main objectives are to improve the power factor (PF) in the boost stage and regulate the output voltage in the buck stage. In the first stage, sliding-mode control is applied to shape the input current according to the rectified voltage, increasing the PF and reducing harmonic distortion. In the second stage, the same control approach is used to maintain a constant output voltage under load variations and disturbances. This study includes the mathematical modeling of both converters, control design, and simulation results in PSIM. The results show that the proposed sliding-mode control strategy effectively enhances energy efficiency, stabilizes the output voltage, and significantly improves the PF, making it suitable for robust and efficient power conversion systems.

*This is an open access article under the [CC BY-SA](https://creativecommons.org/licenses/by-sa/4.0/) license.*



---

## Corresponding Author:

Fredy E. Hoyos

Department of Electrical Energy and Automation, Faculty of Mines

Universidad Nacional de Colombia Sede Medellín

Carrera 80 No. 65 – 223 Medellín, Colombia

Email: fehoyosve@unal.edu.co

---

## 1. INTRODUCTION

Direct-current-to-direct-current (DC-DC) converters are employed to regulate voltage at various stages of power supplies. They are commonly used in renewable energy systems, electric vehicles, and industrial processes. Buck and boost converters are among the most commonly used converters, and they are designed to decrease or increase the input voltage. In addition, these devices require control strategies based on the switching of their electronic switches, usually by adjusting the duty cycle of a pulse-width modulation (PWM) signal, to obtain an acceptable output voltage and be efficient. However, these converters present undesirable behavior under external disturbances or varying load conditions, affecting system stability and energy efficiency [1].

One of the main challenges during the operation of converters is the power factor (PF), particularly when a rectified alternating current (AC) voltage source is used. A low PF implies inefficient energy use, increases the harmonic content in the input current, and negatively affects the operation of electrical components, particularly in demanding industrial environments. PF correction can be performed using boost converters, which are employed to enhance power quality and minimize harmonic distortion. Various methods and innovations have been developed to improve the PF [2], [3]. Interleaved boost converters involve the use of multiple boost converter stages to reduce the inductor volume and weight while

minimizing the input current ripple. Proper current sharing in interleaved configurations is crucial, and control strategies, such as Lyapunov-likelihood techniques, are used to manage it effectively [4]. For three-phase AC/DC boost converters, sliding-mode control (SMC) offers a robust method for achieving a PF greater than 97% through real-time adjustments that compensate for external disturbances and internal uncertainties [5]. Several boost-based topologies, such as three-level boost converters, have been developed for high-power applications with smaller inductors and lower voltage components, improving power density, efficiency, and cost-effectiveness [6]. Techniques such as peak current mode control (PCMC), average current mode control (ACMC), and one-cycle control (OCC) are employed in boost converters to maintain sinusoidal input currents and reduce electromagnetic interference (EMI), particularly in single-phase converters operating in continuous conduction mode [7]. The development of single-stage converters, such as boost-type single-stage resonant PF correction converters, combines boost and resonant conversion in a single topology to simplify the system and enhance efficiency by reducing the number of conversion stages [8]. The combination of flyback and boost converters enables the creation of new single-stage AC/DC converters to achieve a high PF and output regulation using minimal components, leading to improved overall efficiency [9].

Another important challenge is maintaining a stable regulation of the output voltage under sudden load variations to ensure reliable system performance under different operating conditions [10]. An SMC is used to manage the inherent uncertainties of buck converters, such as variable resistive loads and input disturbances. This method ensures continuous conduction mode and voltage stability by suppressing input disturbances and reducing the effects of load variations [11]. In synchronous buck converters, the diode is replaced with a MOSFET, which enhances efficiency over a broad operating range. This is because the MOSFET reduces conduction losses during switching compared to asynchronous designs that traditionally use diodes [12]. Buck converters often incorporate feedback and feedforward control techniques to maintain tight voltage regulation under varying load conditions. These methods are crucial for managing transient responses and ensuring that the buck converter maintains the desired output voltage despite fluctuations in the input voltage or load changes [13]. Advanced applications may use a single-inductor multiple-output (SIMO) configuration, in which one inductor supports multiple independently regulated outputs. This approach minimizes the cost and size of the components, making it suitable for complex systems that require multiple voltage levels [14].

The literature review shows that although multiple studies have individually addressed PF control in boost converters or voltage regulation in buck converters, few studies have integrated both strategies using a common approach. However, the integration of both boost and buck converter stages under a single washout filter has scarcely been addressed in the literature, and most prior studies have focused on single-stage applications (e.g., buck converter only [14]). This integration is especially relevant in cascade architectures or hybrid topologies, where energy efficiency and signal quality are prioritized. Therefore, this study proposes the implementation of a control system composed of two washout filter strategies: a PF controller applied to the boost converter and a voltage regulation controller applied to the buck converter. Unlike previous studies that applied the SMC to each converter independently, this study integrates the SMC based on a washout filter. Many studies have applied SMC techniques to single-stage converters. For example, Ortiz-Castrillón *et al.* implemented SMC in a semi-bridgeless boost converter with PF correction and demonstrated significant improvements over conventional PI control [15]. Similarly, Hamed *et al.* achieved robust voltage regulation in a buck converter using SMC [16]. The dual-stage approach presented in this study provides consistent control behavior, improved robustness, and improved energy efficiency throughout the conversion chain. The performance of the converters was evaluated using Simulink, and the behavior was analyzed in different operating scenarios.

This study aims to contribute to the design of more robust and efficient conversion systems by proposing an SMC-based control architecture that optimizes energy use and improves system stability under real-world operating conditions. The following sections present the mathematical modeling of the converters, the design of an SMC, the results obtained using PSIM, and the conclusions of this study. Unlike most previous studies that address either PF correction or output voltage regulation as independent control problems, this study introduces a unified dual-stage SMC framework based on a washout filter applied simultaneously to both boost and buck converters in a cascaded architecture. The same control philosophy, disturbance rejection mechanism, and stability conditions were employed in both stages, allowing consistent dynamic behavior and modular scalability. To the best of our knowledge, the integration of washout-filtered SMC for simultaneous PF correction and voltage regulation in a boost–buck cascade has not been explicitly reported in the literature. This dual-stage integration is the main novelty of the proposed approach.

## 2. METHOD

Figure 1 shows the closed-loop AC/DC boost-buck converter with PF correction and output voltage regulation. This figure presents a complete schematic implemented in PSIM, including the control blocks, measurement points, and PWM generation. On the left side, the PF correction stage is implemented at the AC input, where a single-phase AC voltage source is followed by a diode bridge rectifier. The objective of this stage is to ensure that the input current ( $I_{in}$ ) remains in phase with the rectified input voltage ( $V_{in}$ ), reducing harmonic distortion and improving the PF.

The central block of the system corresponds to a boost converter that increases the voltage level obtained from the rectifier. In this stage, only the inductor current ( $i_{L1}$ ) is controlled, forcing it to track a reference current generated from the rectified input voltage. The control law of the SMC based on a washout filter provides high robustness against load variations and external disturbances. In the boost converter stage, the voltage of the capacitor is not directly regulated because the regulation is delegated to the subsequent buck stage. On the right side of the system, a buck converter is implemented to step down the voltage supplied by the boost converter and regulate the output voltage according to a desired reference value. Again, an SMC based on a washout filter is applied to the power switch to ensure that the capacitor voltage ( $V_{C2}$ ) remains well-regulated, even under fast and abrupt load changes.

This dual-stage approach enables simultaneous objectives: i) active PF correction at the input of the boost converter and ii) accurate output voltage regulation at the buck converter. With this architecture, different types of loads can be connected to the output while maintaining high energy efficiency and power-quality compliance at the grid interface. The controllers applied in both stages are based on our previous developments of SMCs with a washout filter, as reported and validated in [17]-[20]. These controllers provide high robustness against parameter uncertainties and external perturbations, making them suitable for practical power electronics applications.

The simulation model included a single-phase AC voltage source (10 Vrms, 60 Hz), a full-bridge diode rectifier, a boost converter for PF correction, and a buck converter for output voltage regulation. Both converters operated in the continuous conduction mode and were controlled using an SMC with a washout filter. The switching frequency for both stages was set to 5 kHz, and ideal power switches were considered to focus on the control performance. Voltage and current measurements were obtained using PSIM sensors and fed back to the control blocks, which implemented sliding surfaces and PWM generation.

### 2.1. Control design

Because the system is composed of two connected circuits, the boost circuit receives the input from the AC voltage source with a diode rectifier bridge, and its output is transferred to a buck circuit, which takes this voltage and reduces it according to the reference. Two controls are required to perform two controls, one for each circuit, wherein a slider control (washout) is applied to both sections. The PF was corrected for the boost converter and the output voltage of the circuit for the buck converter.

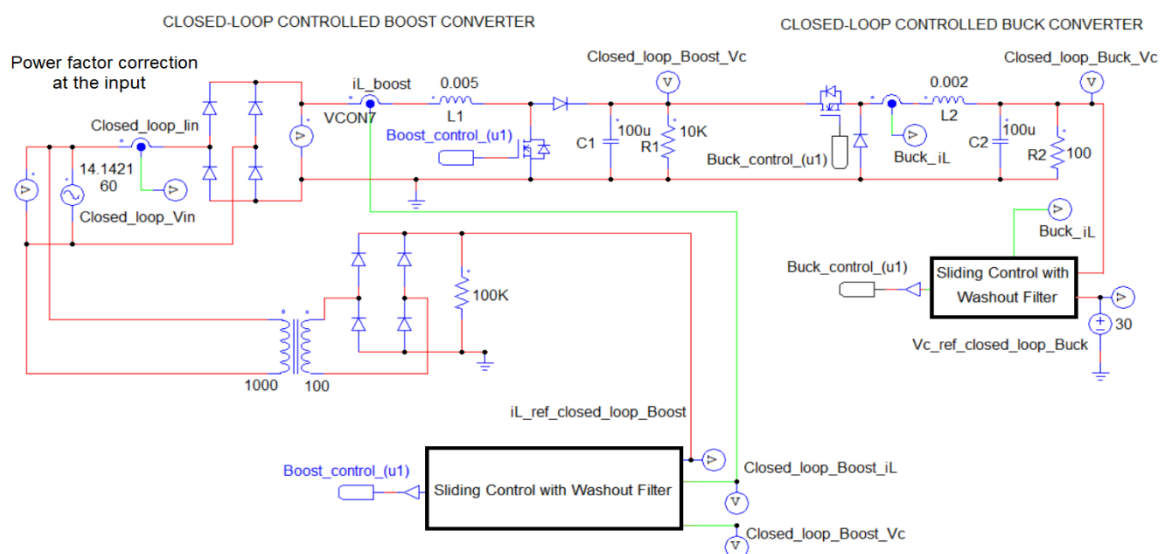


Figure 1. Closed-loop AC/DC boost-buck converter with PF correction and output voltage regulation

## 2.2. Lyapunov stability analysis

A formal Lyapunov-based stability analysis was performed for both converter stages to guarantee global asymptotic stability and robustness against parameter uncertainties. In addition, a practical controller-tuning method is provided to ensure finite-time convergence while mitigating chattering effects. The stability of the proposed SMC strategy was verified using Lyapunov theory. Considering the sliding surface  $s(x) = Cx$ , where  $x$  is the state vector and  $C$  defines the sliding coefficients, the Lyapunov candidate function is chosen as  $V = \frac{1}{2}s^2$ . Its time derivative along the system trajectories is given by  $\dot{V} = s\dot{s}$ . The control law ensures that  $s\dot{s} < 0$  for all operating conditions, which implies asymptotic convergence to the sliding surface and system stability in the sense of Lyapunov. The washout filter contributes to disturbance rejection by attenuating low-frequency components, preserving the sliding condition even under input and load variations. Therefore, the designed control guarantees global stability within the operating range of the converters [21]. To verify the stability of the proposed SMC based on a washout filter in both converter stages, the Lyapunov method was applied using averaged continuous conduction mode (CCM) models [19].

### 2.2.1. Buck converter

The averaged state-space equations are expressed in (1) [20].

$$i_L = \frac{dV_{in}-V_o}{L}, \dot{V}_o = \frac{i_L - \frac{V_o}{R}}{C} \quad (1)$$

The sliding surface is defined by (2).

$$s = c_1(V_o - V_{ref}) + c_2(i_L - i_{ref}) \quad (2)$$

The term  $V_{ref} = 5$  V,  $c_1, c_2 > 0$ , and  $i_{ref} = \frac{V_{ref}}{R}$ . Differentiating  $s$  and substituting the system dynamics yields:

$$\dot{s} = f(x) + b(x)d = c_1 \frac{i_L - \frac{V_o}{R}}{C} + c_2 \frac{dV_{in}-V_o}{L} \quad (3)$$

The control law is expressed in [21].

$$d = d_{eq} - K \text{sign}(s) - \epsilon s \quad (4)$$

The term  $d_{eq} = -\frac{L}{c_2 V_{in}} f(x)$  is the equivalent control. Consider the Lyapunov function  $V = \frac{1}{2}s^2$ . Then:

$$\dot{V} = s\dot{s} = s(-K \text{sign}(s) - \epsilon s) = -K |s| - \epsilon s^2 < 0 \quad (6)$$

Hence, the sliding surface is attractive, and the system is asymptotically stable. Given  $V_{in} = 10$  V,  $L = 1$  mH,  $C = 220$ ,  $R = 10$ , choosing  $K > 0.1$  and  $\epsilon > 0.05$  ensures  $s\dot{s} < 0$ , providing a stable convergence toward the reference voltage.

### 2.2.2. Boost converter

For the boost stage, the averaged model is presented in (6) [20].

$$i_L = \frac{V_{in}-(1-d)V_o}{L}, \dot{V}_o = \frac{(1-d)i_L - \frac{V_o}{R}}{C} \quad (6)$$

The sliding surface used for the PF control is expressed in (7).

$$s = i_L - i_{ref}(t) \quad (7)$$

Where  $i_{ref}(t) = kV_{in}(t)$  is proportional to the rectified voltage to ensure in-phase current and voltage [21]. Its time derivative is expressed in (8).

$$\dot{s} = f(x, t) + b(x)d = \frac{V_{in}-V_o+dV_o}{L} - i_{ref}(t) \quad (8)$$

The control law in (9) was used:

$$d = d_{eq} - K \operatorname{sign}(s) - \epsilon s \quad (9)$$

and the Lyapunov function  $V = \frac{1}{2}s^2$ , the (10) is obtained [21].

$$\dot{V} = s\dot{s} = s(-K \operatorname{sign}(s) - \epsilon s) = -K |s| - \epsilon s^2 < 0 \quad (10)$$

Thus, the reaching condition  $s\dot{s} \leq -\eta |s|$  is satisfied for  $\eta = K > 0$ , ensuring finite-time convergence [20]. The selection  $K > 0.2$  and  $\epsilon > 0.05$  provides adequate robustness against disturbances and parameter variations.

### 2.2.3. Washout filter considerations

Each sliding surface includes a washout filter, as expressed in (11) [21].

$$\dot{w} = \frac{1}{\tau}(s - w), \tilde{s} = s - w \quad (11)$$

The term  $\tau = 1$  ms. The augmented Lyapunov function  $V = \frac{1}{2}\tilde{s}^2$  satisfies  $\dot{V} = -K |\tilde{s}| - \epsilon\tilde{s}^2 < 0$ , confirming global stability of the filtered dynamics and disturbance rejection. According to the Lyapunov-based analysis, both converter stages guarantee global asymptotic stability using the proposed control laws. The washout filter adds a dynamic component that suppresses the steady-state drift and enhances disturbance rejection without compromising stability. These analytical results align with the simulation results, validating the robustness of the proposed SMC based on a washout filter [11], [21].

### 2.3. Controller tuning

The controller parameters were selected to guarantee fast convergence to the sliding surface while maintaining robustness against parameter uncertainties. The proportional gain  $k_1$  and switching gain  $k_2$  were adjusted empirically through simulation, starting from low values to avoid chattering and increasing until a satisfactory transient response was achieved. The washout filter time constant  $\tau$  was chosen to reject low-frequency disturbances without compromising the dynamic response. The tuning process follows the criterion  $k_2 > \frac{f(x)_{max}}{\phi}$ , where  $f(x)$  represents the bounded model uncertainties and  $\phi$  the minimum sliding region width, ensuring  $s\dot{s} < 0$  across all operating points. This procedure provides a practical balance between the robustness, response speed, and stability margins [11], [22].

### 2.4. PF control (boost converter)

Initially, the AC voltage source was rectified by a diode bridge, and the rectified voltage was used as the reference voltage, from which a reference current was generated that had the same shape as the input voltage (rectified half-sinusoidal), which allowed us to search for a PF close to 1. When measuring the current that enters the converter (inductor current), this sample is sent to a subtracting operational amplifier. Subsequently, when both currents (measured and reference) are compared, the error is calculated as shown in (12).

$$error = h(x) = V_C - v_{Cref} + k(i_L - z) = 0 \quad (12)$$

$$u = \begin{cases} u^- = 0, h(x) > 0 \\ u^+ = 1, h(x) < 0 \end{cases} \quad (13)$$

The error signal is converted into a PWM signal that enables the MOSFET to switch, thereby modifying the charge and discharge cycles of the inductor. The greater the error, the higher the duty cycle. Therefore, the measured current was adjusted to be as close as possible to the reference current.

$$\frac{dz}{dt} = w(i_L - z) \quad (14)$$

$$\int dz = \int w(i_L - z)dt \rightarrow z = \int w(i_L - z)dt \quad (15)$$

When the reference current is proportional to the input voltage of the converter, both the current and voltage are in phase, which decreases the harmonics, that is, reduces noise in the system, enables more efficient use of the supplied energy, and brings the PF closer to 1 [23].

**2.5. Voltage control (buck)**

The buck converter also uses an SMC with a washout filter. However, in this case, it incorporates both the measurement of the output voltage and its desired reference, as the main objective is to maintain a constant voltage level. By including this information in the control surface, the responsiveness of the system is improved, allowing for more precise and stable voltage regulation under load variations and dynamic conditions [23].

**3. RESULTS AND ANALYSIS**

This section presents the performance evaluation of the complete power conversion system under two operating conditions. First, the system was analyzed in the open loop, where the boost converter did not implement any current or PF regulation. Subsequently, a closed-loop configuration was tested by applying the proposed SMC with a washout filter to both the boost and buck converters. In all the simulations, the parameters listed in Table 1 were used, and the output voltage reference of the buck converter was set to 30 VDC.

Table 1. System parameters

Parameter	Value
AC input voltage ( $V_{in}$ )	10 VRMS, 60 Hz
Rectifier topology	Single-phase full bridge
Boost inductor (L1)	5 mH
Boost capacitor (C1)	100 $\mu$ F
Boost switching frequency ( $f_{s\_boost}$ )	5000 Hz
Buck inductor (L2)	2 mH
Buck capacitor (C2)	100 $\mu$ F
Buck switching frequency ( $f_{s\_buck}$ )	5000 Hz
Load resistance (R)	100 $\Omega$
Buck reference voltage ( $V_{ref}$ )	30 Vdc
Boost open-loop duty cycle (d)	0.694
Control technique	SMC + washout filter
Simulation software	PSIM

**3.1. System operation in open loop**

Figure 2 shows the system operating with a boost converter in an open loop using a fixed duty cycle ( $d = 0.694$ ) and a switching frequency of 5000 Hz. Under these conditions, only the buck converter was controlled using an SMC based on a washout filter to regulate the output voltage. The input to the system is a (10 V<sub>RMS</sub>), (60 Hz) single-phase source, which is rectified before being fed into the boost stage.

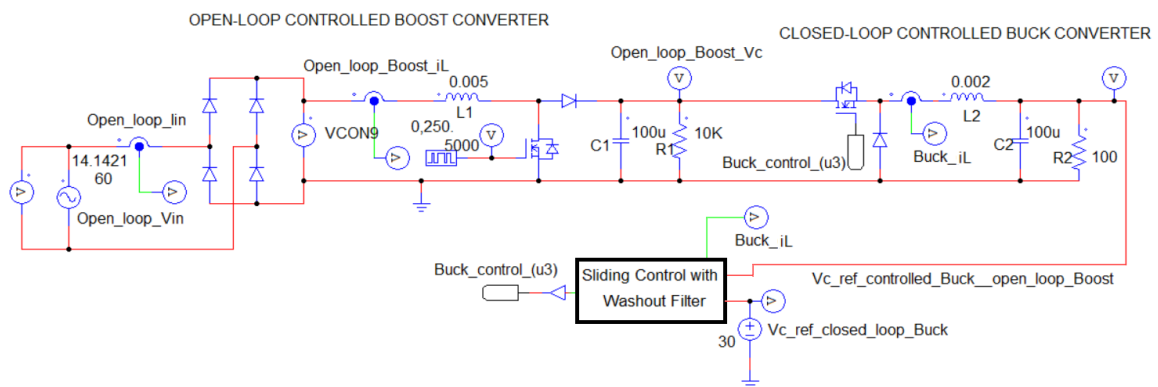


Figure 2. Complete system in open-loop operation (control only applied to the buck stage)

Figure 3 shows the dynamic behavior of the system. In the top waveform, the input voltage ( $V_{in}$ ) (red) and the input current ( $I_{in}$ ) (green). They are clearly out of phase, and the current exhibits a distorted waveform with high harmonic content. This behavior reflects a poor PF and inefficient energy transfer from the AC source. In the second plot, the boost inductor current ( $i_{L1}$ ) shows a pulsating waveform dominated by the rectified input frequency (120 Hz), ranging between 0 and 2.375 A. The discontinuous conduction causes

increased switching stress and contributes to input current distortion. The third plot shows the boost capacitor voltage ( $V_{C1}$ ), which is not regulated in this configuration and therefore exhibits large oscillations between 32.1875 Vdc and 42.1875 Vdc. Such instability in the intermediate DC bus reflects an irregular energy flow and represents a reliability concern for practical implementations. Despite these issues, the bottom plot of Figure 3 shows that the buck output voltage ( $V_{C2}$ ) properly reaches the reference value of 30 Vdc within approximately 5.9375 ms, remaining stable in the steady state with minimum and maximum values of 29.5898 Vdc and 30.0708 Vdc, respectively.

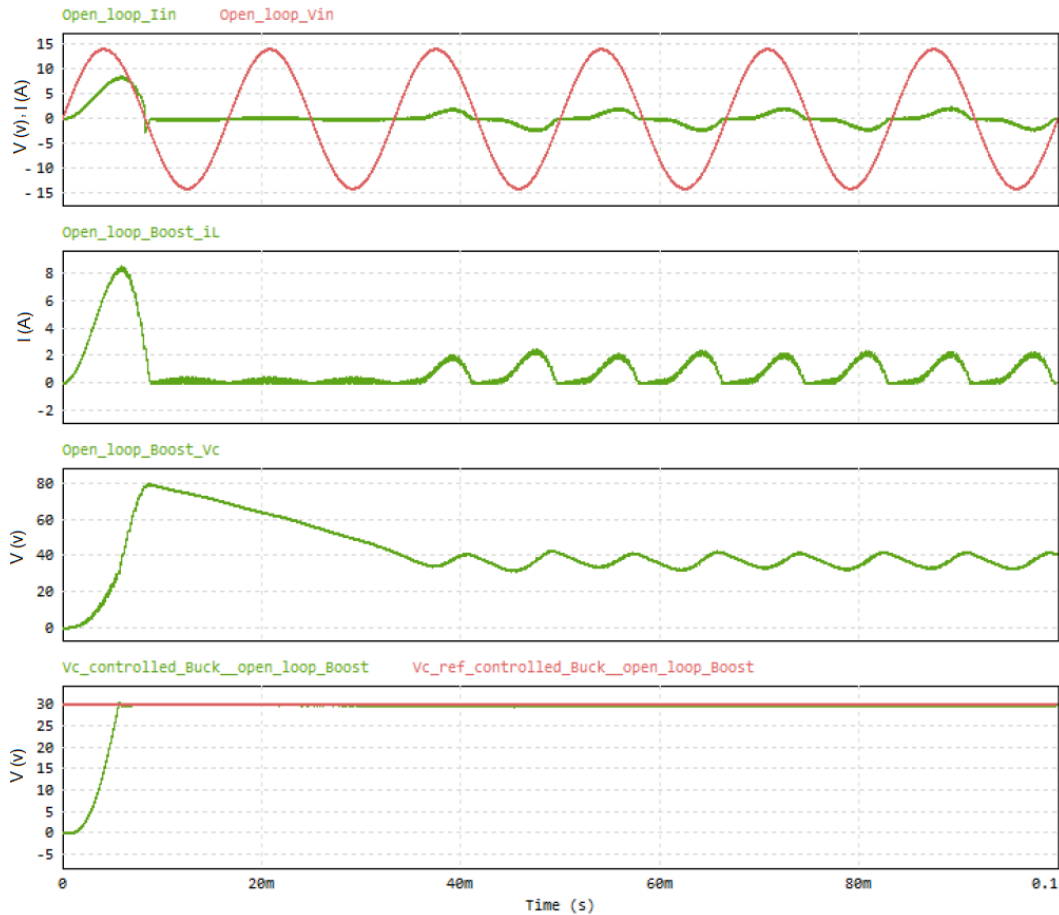


Figure 3. System waveforms in open-loop: ( $V_{in}$ ), ( $I_{in}$ ), ( $i_{L1}$ ), ( $V_{C1}$ ), and ( $V_{C2}$ )

### 3.2. System operation in closed-loop with PF correction

Figure 1 (in Section 2) presents the system under closed-loop operation, where the SMC with a washout filter is applied to both the boost and buck converters. In this case, the boost controller regulates the inductor current ( $i_{L1}$ ) so that the input current becomes sinusoidal and synchronized in phase with the AC voltage, achieving active PF correction. The buck converter continues to regulate the output voltage to the desired reference value.

The simulation results are shown in Figure 4. In the top waveform,  $V_{in}$  and  $I_{in}$  exhibit sinusoidal waveforms at 60 Hz, with zero phase displacement. This confirms a PF close to unity, significantly improving the energy efficiency and reducing the harmonic pollution at the AC interface. In the second plot, the inductor current accurately tracks its full-wave rectified reference, confirming the correct current-shaping operation. Moreover, the current does not fall to zero, which improves the continuity of the power flow and reduces device stress. The third plot shows the boost capacitor voltage ( $V_{C1}$ ), which remains within a stable and acceptable range even without explicit voltage regulation, demonstrating the indirect stabilization effect achieved by the current regulation. The bottom plot shows the buck output voltage ( $V_{C2}$ ) converging to its reference in approximately 37.5 ms, maintaining a steady-state ripple within 29.7656 Vdc and 30.0684 Vdc. This validates the robustness of the buck controller under improved DC link conditions.

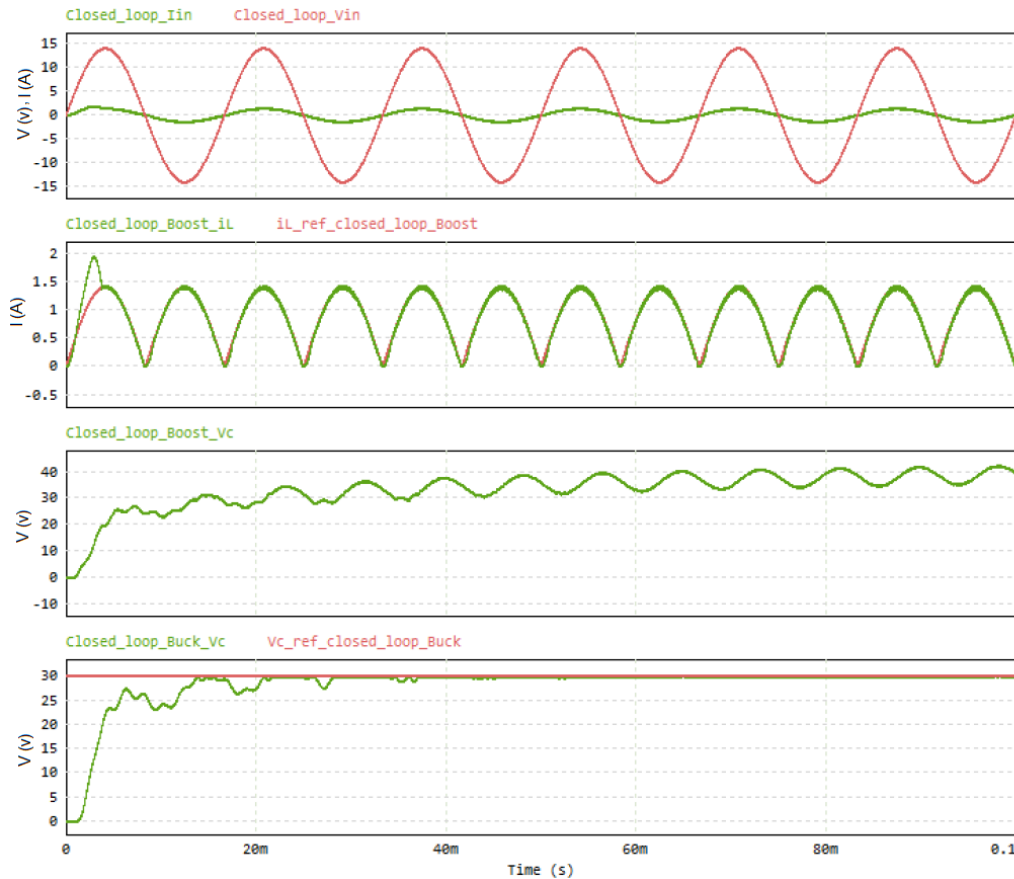


Figure 4. System waveforms in closed loop: ( $V_{in}$ ), ( $I_{in}$ ), ( $i_{L1}$ ), ( $V_{C1}$ ), and ( $V_{C2}$ )

### 3.3. Comparative discussion

Although this study focuses on the SMC based on a washout filter, it is important to consider its relative performance against other strategies. Classical controllers, such as PI and PID, offer simplicity but suffer from limited robustness and slow transient recovery under nonlinear conditions [24]. Intelligent methods, including fuzzy logic and model predictive control (MPC), enhance adaptability but increase computational complexity and tuning requirements [25]. In contrast, the proposed SMC based on a washout filter achieves a balanced trade-off between simplicity, robustness, and dynamic response, as evidenced in [11], [16].

The proposed controller is suitable for real-time deployment on embedded platforms, such as STM32 or TI C2000 DSPs, which provide sufficient processing speed for high-frequency PWM control. Considering a typical switching frequency of 20–50 kHz, a sampling period of less than 10  $\mu$ s, and a PWM resolution of 10–12 bits is sufficient to guarantee a stable sliding motion. The implementation latency, which is dominated by the ADC conversion and interrupt response, can remain below 5  $\mu$ s in optimized firmware, thereby enabling real-time control [26].

Future work will involve implementing the proposed SMC based on a washout filter on a real-time platform to validate its performance. The planned roadmap includes the following: i) Discretization of the control laws for digital execution; ii) Deployment on a DSP or FPGA device, such as the TI TMS320F28379D or Xilinx Zynq, to handle high-frequency switching; iii) Design of signal-conditioning circuits for voltage and current measurements; iv) Implementation of PWM generation and timing synchronization; and v) Experimental validation under varying load conditions. This development will allow the assessment of real-time behavior, efficiency, and robustness, thereby bridging the gap between simulation and hardware realization [27].

Additionally, quantitative power quality and transient performance metrics could be obtained and reported to complement the current analysis. The roadmap includes re-executing the simulation models to extract the total harmonic distortion (THD), conversion efficiency, and load-step recovery time, as well as performing experimental tests on the real-time platform to confirm the results under laboratory conditions. These activities will enable the correlation of simulation and experimental outcomes and provide definitive performance indicators required for future compliance with industrial and power quality standards.

In addition to its dynamic and steady-state performances, the proposed control method contributes to converter reliability. The inherent robustness of the SMC mitigates overcurrent and overvoltage transients, thereby reducing the thermal stress on the power switches. Moreover, the high-frequency switching pattern ensures low EMI susceptibility, improving converter lifespan and compliance with grid-interfacing requirements [28].

The proposed approach can also be extended to multistage converter architectures, such as triple-stage or single-input multiple-output (SIMO) configurations. Due to its modular structure and decoupled washout filter control, the SMC naturally scales to cascaded systems, maintaining robustness and a fast response. Future studies will evaluate these topologies to demonstrate the scalability and modular integration of the controller.

Finally, the proposed design aligns with key industrial standards, including IEEE 519 for harmonic distortion and PF limits, IEC 61000 for electromagnetic compatibility (EMC), and IEC 61800-5-1 for converter safety. The achieved near-unity PF and low current distortion meet the IEEE 519 thresholds, whereas the washout-filtered control contributes to reduced EMI. Future experimental validation will further confirm the compliance margins for the voltage ripple, efficiency, and switching stress [29]-[31].

#### 4. CONCLUSION

This paper presented the design and validation of a boost-buck AC/DC conversion system controlled using an SMC with a washout filter. The main objectives were to achieve active PF correction at the input while maintaining output voltage regulation under load and dynamic variations. Open-loop tests demonstrated the inherent limitations of the system, including the distorted input current, poor PF, and large ripple in the intermediate DC bus. Although the buck converter successfully regulated the output voltage, the overall efficiency and power quality of the system were compromised.

When the proposed control strategy was applied to both conversion stages, the system achieved a PF close to unity with a sinusoidal input current in phase with the AC voltage and a stable DC output of 30 Vdc with a very low ripple. These results confirm the robustness, accuracy, and effectiveness of the SMC based on the washout filter approach for power electronic systems connected to the power grid. Future work will focus on the experimental implementation of the proposed controller and the evaluation of its behavior under real disturbances, nonideal grid conditions, and different load scenarios. Additionally, advanced control techniques can be explored to further improve the dynamic performance and system efficiency.

#### ACKNOWLEDGMENTS

The authors thank the Universidad Nacional de Colombia Sede Medellín for supporting this research.

#### FUNDING INFORMATION

This research received no specific grant from any funding agency in the public, commercial, or not-for-profit sectors.

#### AUTHOR CONTRIBUTIONS STATEMENT

This journal uses the Contributor Roles Taxonomy (CRediT) to recognize individual author contributions, reduce authorship disputes, and facilitate collaboration.

Name of Author	C	M	So	Va	Fo	I	R	D	O	E	Vi	Su	P	Fu
Esteban Flórez Urrego	✓	✓	✓	✓	✓	✓		✓	✓	✓	✓			
Fredy E. Hoyos	✓	✓		✓	✓	✓	✓		✓	✓	✓	✓	✓	
John E. Candelo-Becerra	✓	✓		✓	✓	✓			✓	✓	✓	✓		

C : **C**onceptualization

M : **M**ethodology

So : **S**oftware

Va : **V**alidation

Fo : **F**ormal analysis

I : **I**nvestigation

R : **R**esources

D : **D**ata Curation

O : **O**riting - **O**riginal Draft

E : **E**riting - **R**eview & **E**ditting

Vi : **V**isualization

Su : **S**upervision

P : **P**roject administration

Fu : **F**unding acquisition

**CONFLICT OF INTEREST STATEMENT**

Authors state no conflict of interest.

**DATA AVAILABILITY**

The authors confirm that the data supporting the findings of this study are available within the article. Additional data will be available on request.




**REFERENCES**

- [1] N. Mohan, T. M. Undeland, and W. P. Robbins, *Power Electronics: Converters, Applications, and Design, 3rd Edition*. 2002.
- [2] J. P. M. Figueiredo, F. L. Tofoli, and B. L. A. Silva, "A review of single-phase PFC topologies based on the boost converter," in *2010 9th IEEE/IAS International Conference on Industry Applications - INDUSCON 2010*, IEEE, Nov. 2010, pp. 1–6. doi: 10.1109/INDUSCON.2010.5740015.
- [3] K. Matsui, I. Yamamoto, T. Kishi, M. Hasegawa, H. Mori, and F. Ueda, "A comparison of various buck-boost converters and their application to PFC," in *IEEE 2002 28th Annual Conference of the Industrial Electronics Society. IECON 02*, IEEE, 2003, pp. 30–36. doi: 10.1109/IECON.2002.1187477.
- [4] J. R. Pinheiro, H. A. Grundling, D. L. R. Vidor, and J. E. Baggio, "Control strategy of an interleaved boost power factor correction converter," in *30th Annual IEEE Power Electronics Specialists Conference. Record. (Cat. No.99CH36321)*, IEEE, pp. 137–142. doi: 10.1109/PESC.1999.788993.
- [5] Y. Shtessel, S. Baev, and H. Biglari, "Unity power factor control in three-phase AC/DC boost converter using sliding modes," *IEEE Transactions on Industrial Electronics*, vol. 55, no. 11, pp. 3874–3882, Nov. 2008, doi: 10.1109/TIE.2008.2003203.
- [6] M. T. Zhang, Yimin Jiang, F. C. Lee, and M. M. Jovanovic, "Single-phase three-level boost power factor correction converter," in *Proceedings of 1995 IEEE Applied Power Electronics Conference and Exposition - APEC'95*, IEEE, Nov. 1995, pp. 434–439 vol.1. doi: 10.1109/APEC.1995.468984.
- [7] A. Franco de Souza, E. R. Ribeiro, E. M. Vicente, and F. L. Tofoli, "Experimental evaluation of active power factor correction techniques in a single-phase AC-DC boost converter," *International Journal of Circuit Theory and Applications*, vol. 47, no. 9, pp. 1529–1553, Sep. 2019, doi: 10.1002/cta.2664.
- [8] X. Liu, W. Liu, M. He, W. Wang, Q. Zhou, and J. Xu, "Boost-type single-stage step-down resonant power factor correction converter," *IEEE Transactions on Industrial Electronics*, vol. 68, no. 9, pp. 8081–8092, Sep. 2021, doi: 10.1109/TIE.2020.3013766.
- [9] S. Luo, W. Qiu, W. Wu, and I. Batarseh, "Flyboost power factor correction cell and a new family of single-stage ac/dc converters," *IEEE Transactions on Power Electronics*, vol. 20, no. 1, pp. 25–34, Jan. 2005, doi: 10.1109/TPEL.2004.839876.
- [10] B. Singh, K. Al-Haddad, and A. Chandra, "A review of active filters for power quality improvement," *IEEE Transactions on Industrial Electronics*, vol. 46, no. 5, pp. 960–971, 1999, doi: 10.1109/41.793345.
- [11] J.-F. Tsai and Y.-P. Chen, "Sliding mode control and stability analysis of buck DC-DC converter," *International Journal of Electronics*, vol. 94, no. 3, pp. 209–222, Mar. 2007, doi: 10.1080/00207210601176692.
- [12] H. Eraydin and A. F. Bakan, "Efficiency comparison of asynchronous and synchronous buck converter," in *2020 6th International Conference on Electric Power and Energy Conversion Systems (EPECS)*, IEEE, Oct. 2020, pp. 30–33. doi: 10.1109/EPECS48981.2020.9304966.
- [13] V. W. Ng and S. R. Sanders, "A High-Efficiency Wide-Input-Voltage Range Switched Capacitor Point-of-Load DC-DC Converter," *IEEE Transactions on Power Electronics*, vol. 28, no. 9, pp. 4335–4341, Sep. 2013, doi: 10.1109/TPEL.2012.2224887.
- [14] M. Belloni *et al.*, "A 4-output single-inductor DC-DC Buck Converter with Self-Boosted Switch Drivers and 1.2A Total Output Current," in *2008 IEEE International Solid-State Circuits Conference - Digest of Technical Papers*, IEEE, Feb. 2008, pp. 444–626. doi: 10.1109/ISSCC.2008.4523248.
- [15] J. R. Ortiz-Castrillón, S. D. Saldarriaga-Zuluaga, N. Muñoz-Galeano, J. M. López-Lezama, S. Benavides-Córdoba, and J. B. Cano-Quintero, "Optimal sliding-mode control of semi-bridgeless boost converters considering power factor corrections," *Energies*, vol. 16, no. 17, p. 6282, Aug. 2023, doi: 10.3390/en16176282.
- [16] S. B. Hamed, M. Ben Hamed, and L. Sbata, "Robust voltage control of a buck DC-DC converter: a sliding mode approach," *Energies*, vol. 15, no. 17, p. 6128, Aug. 2022, doi: 10.3390/en15176128.
- [17] M. Monsalve-Rueda, J. E. Candelo-Becerra, N. Toro García, and F. E. Hoyos Velasco, "Experimental validation of a non-linear sliding-mode control based on a washout filter applied to microgrids," *International Review of Automatic Control (IREACO)*, vol. 13, no. 4, p. 162, Jul. 2020, doi: 10.15866/ireaco.v13i4.17672.
- [18] M. Monsalve-Rueda, J. E. Candelo-Becerra, and F. E. Hoyos, "Second-order sliding-mode control applied to microgrids: DC & AC buck converters powering constant power loads," *Energies*, vol. 17, no. 11, p. 2701, Jun. 2024, doi: 10.3390/en17112701.
- [19] H. Velasco-Muñoz, J. E. Candelo-Becerra, F. E. Hoyos, and A. Rincón, "Speed regulation of a permanent magnet DC motor with sliding mode control based on washout filter," *Symmetry*, vol. 14, no. 4, p. 728, Apr. 2022, doi: 10.3390/sym14040728.
- [20] M. Monsalve-Rueda, J. E. Candelo-Becerra, and F. E. Hoyos, "Dynamic behavior of a sliding-mode control based on a washout filter with constant impedance and nonlinear constant power loads," *Applied Sciences*, vol. 9, no. 21, p. 4548, Oct. 2019, doi: 10.3390/app9214548.
- [21] Y. Shtessel, C. Edwards, L. Fridman, and A. Levant, *Sliding Mode Control and Observation*. in Control Engineering. New York, NY: Springer New York, 2014. doi: 10.1007/978-0-8176-4893-0.
- [22] A. Levant, "Chattering Analysis," *IEEE Transactions on Automatic Control*, vol. 55, no. 6, pp. 1380–1389, Jun. 2010, doi: 10.1109/TAC.2010.2041973.
- [23] D. W. Hart, *Power Electronics*. McGraw-Hill, 2011.
- [24] A. Das and M. K. Namboothiripad, "Voltage control of buck converter using sliding mode controller," *International Journal of Engineering Research & Technology*, vol. 3, no. 4, pp. 1619–1623, 2014.
- [25] H. S. Zad, A. Ulasyar, A. Zohaib, M. Irfan, S. A. Haider, and Z. Yaqoob, "Adaptive sliding mode control of DC-DC buck converter with load fluctuations for renewable energy systems," in *ICAME 2024*, Basel Switzerland: MDPI, Sep. 2024, p. 10. doi: 10.3390/engproc2024075010.




- [26] M. P. Kazmierkowski, R. Krishnan, and F. Blaabjerg, Eds., *Control in Power Electronics*. Elsevier, 2002. doi: 10.1016/B978-0-12-402772-5.X5000-5.
- [27] H. El Alami *et al.*, “FPGA in the loop implementation for observer sliding mode control of DFIG-generators for wind turbines,” *Electronics*, vol. 11, no. 1, p. 116, Dec. 2021, doi: 10.3390/electronics11010116.
- [28] J. Holtz, “Pulsewidth modulation for electronic power conversion,” *Proceedings of the IEEE*, vol. 82, no. 8, pp. 1194–1214, 1994, doi: 10.1109/5.301684.
- [29] “IEEE recommended practice and requirements for harmonic control in electric power systems,” Mar. 27, 2014, *IEEE, Piscataway, NJ, USA*. doi: 10.1109/IEEESTD.2014.6826459.
- [30] International Electrotechnical Commission, *IEC 61000-6-4:2018: Electromagnetic Compatibility (EMC) – Part 6-4: Generic Standards – Emission Standard for Industrial Environments*, Geneva, Switzerland: IEC, 2018.
- [31] International Electrotechnical Commission, *IEC 61800-5-1:2022: Adjustable Speed Electrical Power Drive Systems – Part 5-1: Safety Requirements – Electrical, Thermal and Energy*, Geneva, Switzerland: IEC, Aug. 2022.

## BIOGRAPHIES OF AUTHORS






**Esteban Flórez Urrego**    was an assistant teacher of Electrical Circuits Analysis in 2023 at the Universidad Nacional de Colombia Sede Medellín. He received a B.S. degree in Control Engineering from the same institution in 2025. His undergraduate research focused on the control systems for power converters and intelligent automation. After graduation, he began working in the fields of process automation, data analytics, and software development, integrating control theory with industrial digitalization technologies. His research interests include power electronics, embedded control, real-time systems, and the application of data-driven methods for industrial process optimization. He has participated in academic and applied projects related to energy efficiency, Internet of Things (IoT) platforms, and control algorithms. His current professional activities focus on developing automation solutions and analytical tools to enhance the operational performance of industrial systems. He can be contacted at email: [eflorezu@unal.edu.co](mailto:eflorezu@unal.edu.co).



**Fredy E. Hoyos**    from La Cruz, Nariño, Colombia, received his B.Sc. and M.Sc. degrees in Electrical Engineering and Industrial Automation from Universidad Nacional de Colombia, Manizales, Colombia, in 2006 and 2009, respectively, and his Ph.D. in Engineering with emphasis on Automation in 2012. Dr. Hoyos is currently a Full Professor at the Faculty of Mines, Department of Electrical Energy and Automation, Universidad Nacional de Colombia, Medellín Campus. He is the Director of the A1-rated research group “Digital Signal Processing for Real-Time Systems” in Minciencias. His research interests include nonlinear control, real-time systems, non-smooth dynamics, power electronics, and sliding-mode control applied to power converters and technological processes. He can be contacted at email: [fehoyosve@unal.edu.co](mailto:fehoyosve@unal.edu.co).



**John E. Candelo-Becerra**    received his B.S. in Electrical Engineering in 2002 and his Ph.D. in Engineering with an emphasis on Electrical Engineering in 2009 from the Universidad del Valle, Cali, Colombia. His employment experience includes working at the Empresa de Energía del Pacífico EPSA, Universidad del Norte, and Universidad Nacional de Colombia Sede Medellín. He is currently a professor (full) at the Universidad Nacional de Colombia Sede Medellín. His research interests include engineering education, planning, operation, and control of power systems, artificial intelligence, and smart grids. He is a senior researcher at MinCiencias and a member of the Applied Technologies Research Group, GITA, at the Universidad Nacional de Colombia. He can be contacted at email: [jecandelob@unal.edu.co](mailto:jecandelob@unal.edu.co).